COMPARATIVE ANALYSIS OF TWO PROTOCOLS OF MOUSE TISSUES DECELLULARIZATION FOR APPLICATION IN EXPERIMENTAL ONCOLOGY

A.D. Pospelov[1*], *L.B. Timofeeva*[1, 2], *E.I. Cherkasova*[1], *I.V. Balalaeva*[1]

[1] Institute of Biology and Biomedicine, Lobachevsky State University of Nizhny Novgorod, 23 Gagarin ave., Nizhny Novgorod 603950, Russia;
[2] Privolzhsky Research Medical University, 10/1, Minin and Pozharsky Sq., Nizhny Novgorod, 603950, Russia
eso103163@gmail.com (A.D.P.); bioli@mail.ru (L.B.T); cherkasova.el@yandex.ru (E.I.C.); irin-b@mail.ru (I.V.B)

Abstract. Decellularized matrices of animal organs can serve as a promising platform for creating highly relevant three-dimensional in vitro models of tumor growth. In this work, the applicability of two decellularization protocols for obtaining the extracellular matrices of various murine organs was examined. The resulting decellularized matrices were characterized by visual integrity and preservation of the tissue architectonics. A high degree of the cellular component elimination was demonstrated while maintaining the basic structures of the extracellular matrix. From the point of view of convenience and ease of use, as well as the quality of the obtained matrices, the method based on the use of detergent sodium dodecyl sulfate and trypsin-aprotinin complex has demonstrated the greatest suitability. In the future, the developed protocol will be used to study tumor-matrix interaction and tissue-specific characteristics of growth and morphology of tumor cells.

Keywords: 3D in vitro tumor models, decellularization, extracellular matrix, murine models of tumor growth.

List of abbreviations

SDS – sodium dedecylsulfate
SDC – sodium deoxycholate
ECM – extracellular matrix
DCL – decellularization/decellularized
Tr-Ap – trypsin-aprotinin
Nuc – nucleases

Introduction

Elucidation of the hallmarks and regularities of carcinogenesis and further tumor progression is among the key issues in modern fundamental medicine. Establishment of the molecular and cellular mechanisms underlying carcinogenesis is the basis for the development of practical methods for the treatment of oncological diseases. Research in cancer biology requires the creation of relevant models of tumor growth, both *in vivo* (tumor-bearing animals) and *in vitro*. Obtaining of *in vivo* tumor models using laboratory animals has limitations due to the bioethical aspect; in addition, the complexity of such models makes it difficult to interpret the results in relation to the molecular mechanisms of the observed processes. As a simpler and more humane alternative, many three-dimensional *in vitro* tumor models are currently being developed. Such models should ideally recapitulate the features of the three-dimensional structure of the tumor, including the presence of gradients of nutrients, gases and metabolites, as well as cell-cell and cell-matrix interactions.

The extracellular matrix (ECM) is a complex polymeric structure consisting of compounds such as collagens, proteoglycans, glycosaminoglycans, etc (Hoshiba et al., 2016). The functions of the extracellular matrix include tissue morphogenesis, differentiation of resident cells, implementation of mechanical properties of tissue and macromolecular filtration(Frantz et al., 2010). The composition and structure of the extracellular matrix are specific for each type of tissue and organ and determine the tissue-specificity of cellular functions (Hoshiba et al., 2010). Importantly, the extracellular matrix plays an active role in the development of tumors (Lee et al., 2019; Lu et al., 2012). The progression of tumors is greatly influenced by both mechanical and chemical signals from the extracellular matrix, which complements the genetic changes in malignant cells (Crotti et al., 2017). For example, an increase in the rigidity of the extracellular matrix can enhance integrin-

mediated interactions between cells and the extracellular matrix, which leads to an increase in the tension of the cytoskeleton and activation of a number of internal transformations in the cell (Canel et al., 2013).

To date, many different matrix-based 3D models of tumor growth *in vitro* have been proposed, in the overwhelming majority of which artificial hydrogels from natural (collagen, hyaluronic acid) or synthesized polymers are used (Hashimoto et al., 2019; Piccoli et al., 2018; Sokolova et al., 2019). Decellularized (DCL) matrices of animal organs can serve as a promising platform for creating more relevant matrix-containing models. Among their advantages are the authenticity of the molecular composition characteristic of a particular organ and the preservation of tissue architectonics, which allows simulating the processes of tumorigenesis with a high degree of proximity (Erdogan & Webb, 2017; Varol & Sagi, 2018).

There are a large number of decellularization methods, including the treatment of the original tissue with detergents, enzymes, or with the use of physical impact. Most of the protocols are based on the use of sodium dodecyl sulfate (SDS) and Triton X-100 (Fernández-Pérez & Ahearne, 2019; Simsa et al., 2018). It should be noted, that the choice of detergent, as well as the time of decellularization, affect the residual composition and structural integrity of the extracellular matrix proteins, as well as the cytotoxicity of the resulting matrix (Fu et al., 2014; White et al., 2017). Thus, the creation of a tissue construct that has a high degree of the natural microenvironment recapitulatuion, preserves the appropriate spatial complexity and the ability to maintain cell functionality, is of great importance for further applicability of the matrix.

It is worth noting that the vast majority of the protocols reported are developed for either human organs or the organs of large mammals due to the initial development of DCL matrices technologies for regenerative medicine. In experimental oncology, small rodents (e.g. mice and rats) are the classic objects of study. At the same time, works concerning DCL techniques for small animal's organs are scarce, and the proposed procedures have been tested for individual organs, i.e. no universal protocols were still established. In this work, we demonstrated the possibility of using chemical-enzymatic protocols based on chemical detergents (SDS, Triton-X100) in combination with the proteolytic enzyme trypsin or nucleases to obtain DCL matrices of kidneys, liver, spleen, skin, ovaries, and lungs of mice.

Materials and Methods

Laboratory animals

The work was carried out on BALB/C mice (females, weight 20–23 g) obtained from the SPF vivarium of the Lobachevsky State University of Nizhny Novgorod (UNN). The animals were housed under standard conditions (at 25–26 °C and 12 h light-dark cycle) supplied with food and water ad libitum. All research procedures were reviewed and approved by the Bioethics Commitee of UNN (protocol No15 from 02.15.2018). Animals were exposed to general anesthesia and euthanized by cervical dislocation.

Organ harvesting

The euthanized animals were trimmed to remove hair and treated with 96% ethanol for antiseptic purposes. Autopsy was performed in a laminar flow cabinet with sterilized instruments to maintain sterility of the tissue samples. Segments of skin, liver, kidney, ovaries, lungs and spleen were collected from each animal. The heart/lungs/thymus complex was extracted simultaneously and then separated. Each organ was freed from fat adhesions. The collected organs were rinsed with normal saline and were placed into a primary decellularizing medium to obtain an organ matrix. The scheme of the experimental procedure is presented in Fig. 1.

Decellularization of the mouse organs

To maintain sterility, all decellularizing media and labware were autoclaved at 120 °C under 1 atm for 1 h. Antibiotic-antimycotic namely 1×penicillin-streptomycin 80 mkg/ml + amphotericin B 5 mkg/ml (PanEco, Russia) was added to each type of the media. The entire decellularization process was carried out on an orbital shaker with a rotation speed of 120 rpm.

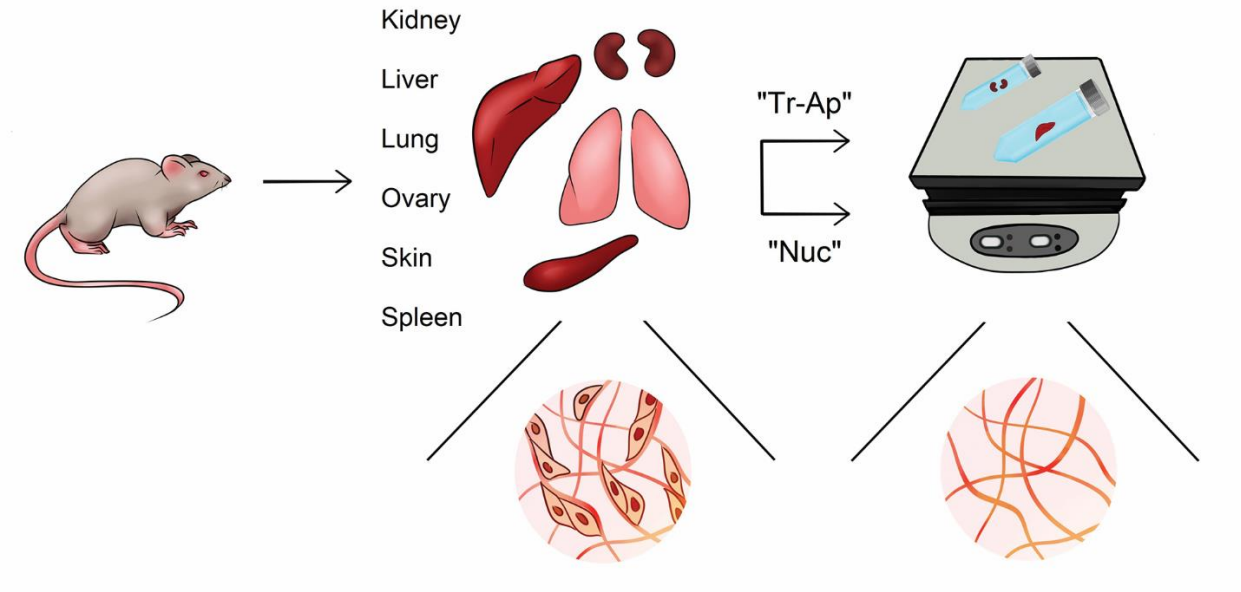

Fig. 1. Simplified scheme of decellularization. Segments of skin, liver, kidney, ovaries, lungs and spleen were collected from each animal. Two different protocols of chemical-enzymatic decellularization were applied to each of the organs: «Tr-Ap» – trypsin-aprotinin based protocol, «Nuc» – nuclease based protocol. To analyze the performance of the decellularization, hystomorphological analysis of the initial organs and resulting matrices was performed

Two different protocols of chemical-enzymatic decellularization were applied to each of the organs harvested.

Trypsin-aprotinin based decellularization. The extracted organs were washed in sterile distilled water. The organs were then proceeded to a series of successive incubations in 1% Triton X-100 (Helicon, Russia) with 1×antibiotic-antimicotic (2 h), distilled water (1 h), 0.5% trypsin – 0.2% EDTA solution (PanEco, Russia) (1 h). To neutralize the action of trypsin on collagen fibers, the organs were then incubated in 0.8 mg/ml solution of trypsin inhibitor aprotinin (Thermo Fisher, USA) for 1 h. After that decellularization was continued by the successive incubation of organs in 0.5% SDS solution (Panreac, USA) (24 h) and 0.5% Triton X-100 solution (12 h).

Nuclease based decellularization. The organs were prepared as described above and proceeded to successive incubations in 10 mM Tris-HCl – 0.1 mM EDTA solution (PanEco, Russia), pH 8.0 at 5°C (48 h), 3% Triton X-100 at room temperature (48 h) and 0.03 mg/ml RNAse A (Thermo Fisher, USA) and 3.3 UI/ml DNAse 1 (Thermo Fisher, USA) for 24 h.

Hystomorphological analysis

Histological cassettes with organ samples or DCL matrices were placed in a neutralized 10% formalin solution for 24 h at room temperature. Samples were washed from excess fixative, dehydrated and embedded in paraffin according to the standard protocol. 7 μm-thick slices were further dewaxed, stained with hematoxylin-eosin (Biovitrum, Russia) (Mayer's hematoxylin; eosin 1% aqueous solution) according to the manufacturer's instructions, and enclosed in Canadian balsam (Panreac, USA). Alternatively, the slices were stained with acridine orange (PanEco, Russia) as follows: washed with 0.2 M sodium acetate buffered solution, pH 4.2, stained with 0.1% acridine orange for 10 min in the dark, washed with distilled water and 0.2 M sodium acetate, and embedded in sodium acetate buffered solution. Images were obtained

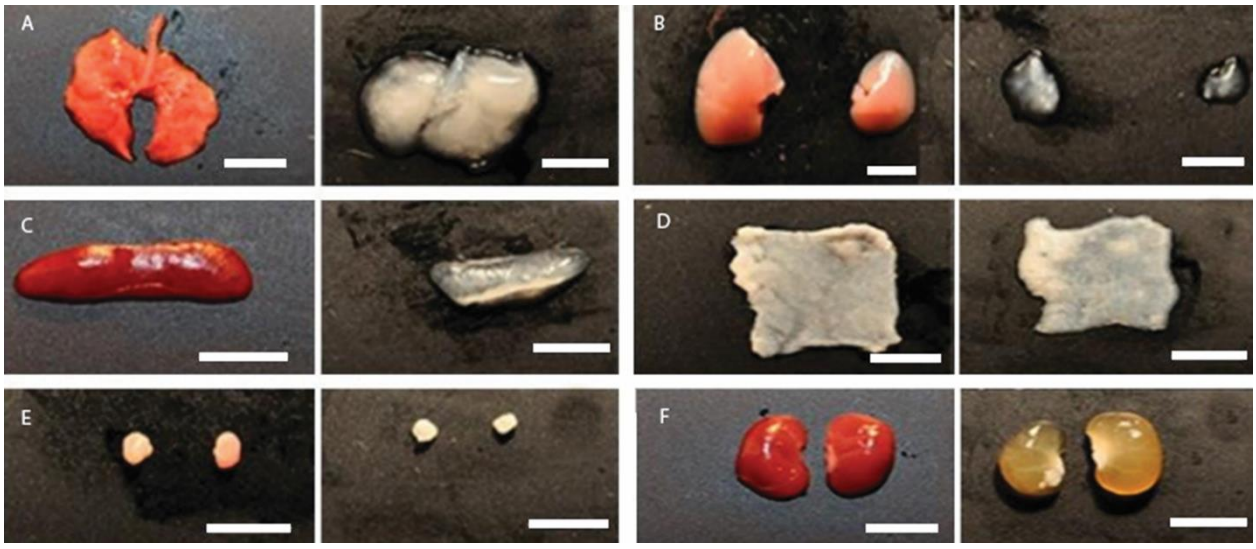

Fig 2. Visual comparison of lungs (A), liver (B), spleen (C), skin (D), ovaries (E) and kidneys (F) of mouse after decellularization based on «trypsin-aprotinin» protocol. Bar size – 5 mm

using Axio Observer Z1 LSM 710 NLO/Duo laser scanning microscope (Carl Zeiss, Germany) with an EC Plan-Neofluar 20×/0.5 objective lens. The fluorescence of acridine orange was excited with 458 nm laser and fluorescent signal was detected in the range of 505–552 nm.

Results

Most of the currently existing protocols for obtaining DCL-matrices are based on the use of sodium dodecyl sulfate (SDS). We have tested a simple protocol based on 1% SDS in preliminary experiments, but extremely strong degradation of the matrices microstructure (data not shown) indicates its inapplicability for murine organs.

To improve the matrices quality, we formulated two original DCL protocols. The first one implicates using SDS in a lower concentration in combination with other decellularizing agent, trypsin («trypsin-aprotinin» protocol). According to the published reports it might facilitate cell debris removal from the depths of dense tissues (DeQuach et al., 2010). Trypsin was chosen due to its protease activity; it induces constriction of matrix fibers, which facilitates cellular elimination (Brown et al., 2011). To neutralize the effect of trypsin on the components of the extracellular matrix, its inhibitor, aprotinin, was applied. For the second protocol, Triton X-100 was chosen as the main detergent, as it removes cell structures more gently than SDS (Shupe et al., 2010); and for the final elimination of the antigenic component RNAse A and DNAse 1 were added (‘nucleases-based’ protocol) (Yang et al., 2009). Since the volume of the selected murine organs does not exceed cubic centimeter, we have chosen the technique of organ incubation in a washing decellularizing solution.

Both of the developed protocols allowed us to obtain DCL matrices of murine kidney, spleen, skin, liver, lungs, and ovaries (Fig. 2). Initial visual assessment showed a strong decrease in the volume of the resulting matrices relative to initial organs. Samples were almost completely discolored after application of both protocols, except for dense organs such as kidney and liver, where a dark core could be observed. It should be mentioned, that discoloration testifies a decrease in cell abundance. To identify the difference between normal and decellularized organs and to assess a degree of the ECM structure preservation in decellularized tissues, histomorphological analysis has been performed.

The main component of kidney tissue is the nephron, which consists of the renal corpuscle and the nephron canal. The renal corpuscle includes a capillary glomerulus and an epithelial capsule; the nephron canal is an epithelial tube. Thin connective tissue layers with blood vessels are located between the elements of the nephron (Fig. 3A). Decellularization of the kidney by the trypsin-aprotinin complex leads to significant tissue compression (Fig. 3B). The cell component is not detectable. In the matrix, structures characteristic of the kidney are distinguishable: renal corpuscles and the nephron canal. After decellularization with nucleases, a certain number of cells are retained in the kidney tissue and found both under hematoxylin-eosin (Fig. 3C) and acridine orange staining (Fig. 4A). The integrity of the collagen fibers is compromised.

The spleen consists of a parenchyma, represented by formed elements of blood, and a reticular stroma. In the parenchyma, white and red pulps are distinguished. White pulp, or lymph nodules, are collections of lymphocytes. All types of blood cells are present in the red pulp, predominantly erythrocytes (Fig. 3D). The spleen matrix after decellularization with trypsin-aprotinin protocol is a cell-free ECM mass lacking characteristic structures (Fig. 3E). When stained with acridine orange, cells are not detected. After decellularization with nucleases, lymph nodules are visible on hematoxylin-eosin stained samples, around which the matrix is fragmented, which indicates the disruption of fibers integrity. The nodules have a granular structure due to the accumulation of eliminated cells (Fig. 3F).

Normally, the dermis of the skin is represented by dense connective tissue, the main component of which is collagen fibers. Fibers form bundles between which connective tissue cells are located (fibroblasts, fibrocytes, etc.). In addition, the dermis contains hair follicles, which are a hair shaft surrounded by an epithelial sheath. Sebaceous glands are located next to the follicles (Fig. 3G). After decellularization, cells were not detected in a skin sample treated with trypsin-aprotinin protocol when stained with hematoxylin-eosin. The structure of the extracellular matrix is significantly disrupted, no fibers are observed. Remaining hair follicle structures are represented only by the hair shaft (Fig. 3H). In a skin sample treated with nucleases hematoxylin-eosin staining indicates all structures characteristic of the dermis of the skin, including cellular elements (nuclei of connective tissue cells, epithelial cells, cells of the sebaceous glands). Swelling of collagen fibers is observed (Fig. 3I).

The structural components of the liver are lobules and interlobular structures – portal triads and collecting veins. The lobules consist of hepatocytes, organized in the hepatic tracts, between which capillaries are located, collecting in the center of the lobule into the central vein. The connective tissue component of the liver is poorly developed and is concentrated mainly around the interlobular structures (Fig. 3J). In the liver tissue after decellularization with the trypsin-aprotinin complex, all characteristic structures are visualized, including hepatocytes, some of which do not contain nuclei, and the endothelium lining the interlobular vessels. Inside the lobule, the radial organization is partially broken due to the destruction of hepatocytes (Fig. 3K). Hematoxylin-eosin staining of tissue decellularized with nucleases demonstrates the absence of cells in the central region of the sample, while small dark randomly located rounded nuclei are observed along the periphery (Fig. 3L). Acridine orange staining also demonstrates the presence of cell groups (Fig. 4B).

Lung tissue is made up of numerous alveoli, blood vessels of various sizes and airways, represented by bronchi and bronchioles. All of these structures are lined with epithelial tissue, under which connective tissue elements are present in varying amounts (Fig. 3M). After decellularization by the trypsin-aprotinin complex, the cellular component of the lung tissue is completely absent both in case of hematoxylin-eosin (Fig. 3N) and acridine orange staining. The structure of the matrix is significantly changed due to the strong swelling of collagen fibers, the alveoli are indistinguishable. During decellularization by nucleases, the alveoli, pulmonary passages and bronchioles are visualized

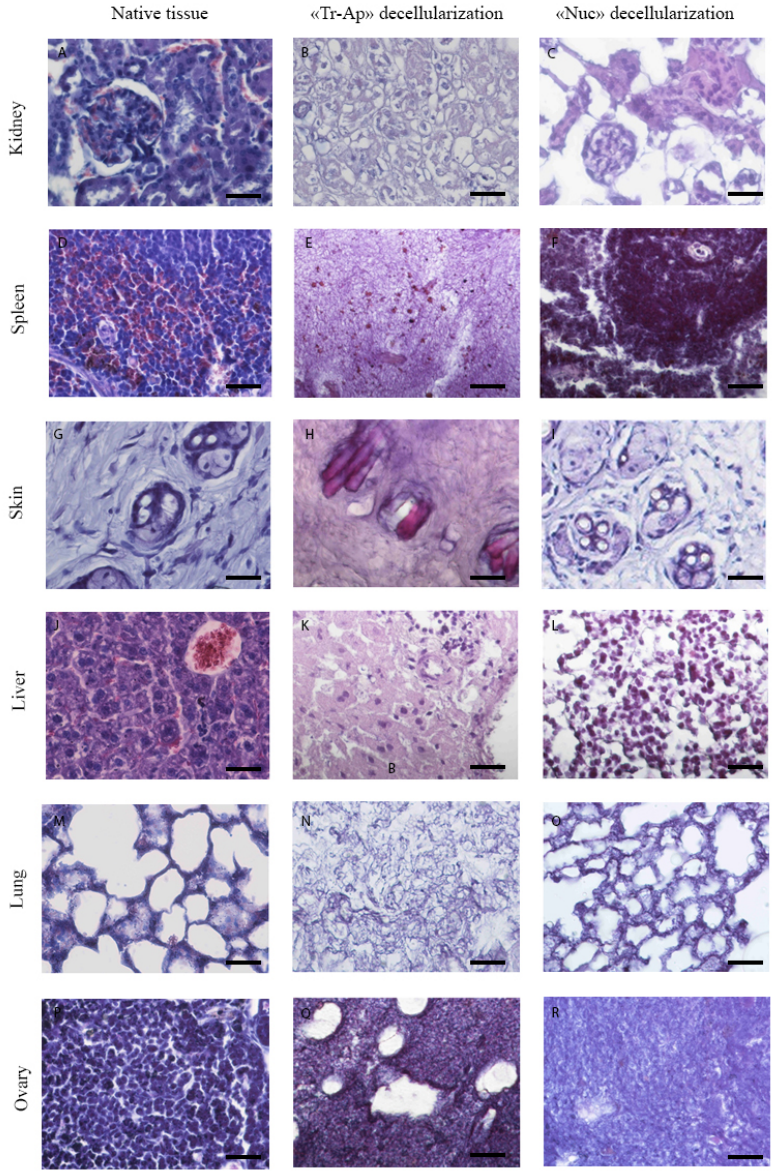

Fig. 3. Hematoxylin-eosin staining of decellularized matrices of murine kidney, spleen, skin, liver, lung and ovary obtained by 'trypsin-aprotinin' and 'nucleases-based' protocols compare to normal tissues. Bar size – 100 μm

in the matrix of the lung tissue, which indicates a high degree of its preservation. Staining both with hematoxylin-eosin (Fig. 3O) and acridine orange, no cellular elements were observed.

The outside of the ovary is covered with a dense connective tissue membrane. Underneath is the cortex, which contains follicles at different stages of maturation. The connective tissue between the follicles contains fibroblasts. Under the cortical substance is the medulla, represented by loose connective tissue with blood vessels (Fig. 3P). The matrix decellularized by the trypsin-aprotinin complex is a heterogeneous network of fibers with an uneven fiber density. In place of a part of the follicles, voids are observed, in the place of others – eliminated

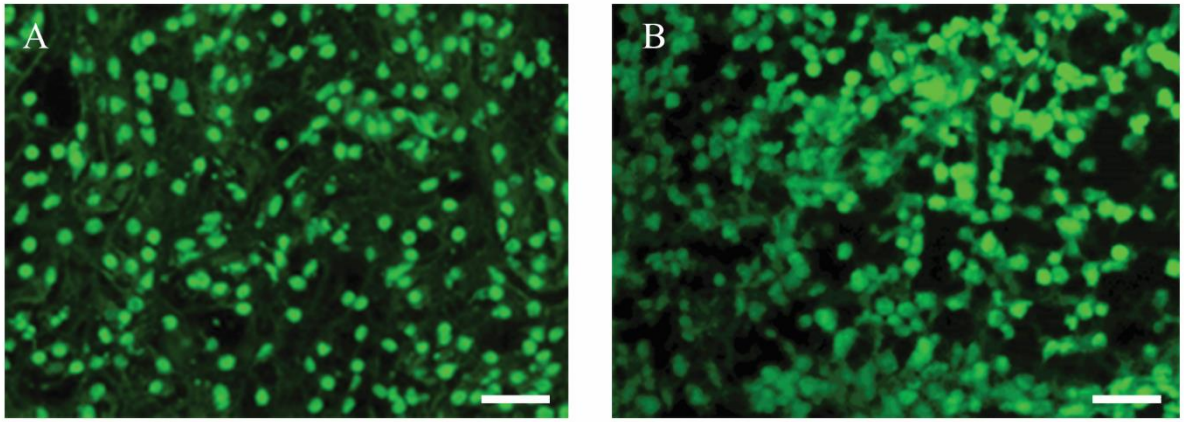

Fig. 4. Acridine orange staining of residual cells in the core of liver (A) and kidney (B) obtained by 'nucleases-based' protocol. Bar size – 100 μm

Table 1

The comparison of main characteristics of decellularizing protocols

Method	Time needed	Simplicity of the method	Degree of cell component elimination	Visual integrity	Degree of matrix integrity
Trypsin-aprotinin	41 hrs	medium	high	medium	high
Nucleases-based	120 hrs	easy	medium	high	medium

cells of the follicular epithelium (Fig. 3Q). Cells are not detectable with any of the staining methods used. After decellularization with nucleases, the matrix is represented by a dense network of fibers with voids in place of follicles (Fig. 3R). Cellular elements are not observed with any of the staining protocols.

To compare the applicability of particular method, each method was analyzed by a list of factors, such as time consuming, practical simplicity of method, degree of cell elimination and matrix integrity (*via* histomorphological staining) and by visual integrity of decellularized organs (Table 1).

Discussion

Using two original protocols of murine organ decellularization, we obtained matrices of six organs and analyzed their properties. The choice of the organs was made for a number of reasons. lungs, liver and spleen were chosen as main targets for metastatic tumors formation (Robinson et al., 2017; Roett & Evans, 2009); the ovary was added to this list with a view to follow-up study of ovarian cancer metastasis. Kidneys and skin at the contrary were taken for diversity of composition and structure of ECM.

Different organs demonstrated different integrity of the resulted matrix. It is can be explained by the different chemical composition and architectonics of the matrices as well as different cells-to-matrix proportions (Kai et al., 2019). For instance, skin, with a high concentration of collagen fibers compare to the spleen, showed less resistance to the SDS based protocol. At the same time, nuclease-based protocol without SDS was inapplicable for washing out the core cells in organs with a high cell density, such as liver and kidneys (Fig 4.).

Changes in the structural features of native matrix fibers can lead to changes in the rigidity of the entire matrix. This variability in the stiffness modulus has a high impact on subsequent cell repopulation(Gilkes et al., 2014) (link). Some researchers rise attention to the relationship between the invasive potential of tumor cells and the mechanical properties of matrix fibers (Wullkopf et al., 2018) (link). Thus, it can

be argued that the influence of the features of the decellularization protocols on the properties of the resulting matrix is of great importance for subsequent work on recellularization.

The results of the study show that the protocol based on the use of the low-concentration SDS and trypsin-aprotinin complex is more applicable, most correctly preserving the microstructure of the matrix (Table 1.). It should be noted that in each individual case it was necessary to seek a compromise between the completeness of cell elimination and the preservation of the structure and properties of the matrix itself.

To conclude, two original protocols were experimentally compared, which made it possible to obtain decellularized matrices of different murine organs such as kidneys, liver, lungs, spleen, skin and ovary. From the point of view of convenience and ease of use, as well as the quality of the obtained scaffolds, the method based on the use of SDS and trypsin-aprotinin complex has demonstrated the greatest suitability. In the future, the developed protocol will be used to study tumor-matrix interaction and tissue-specific characteristics of growth and morphology of tumor cells.

Acknowledgments

This research was funded by the Russian Science Foundation (project No. 19-74-20168).

References

BROWN, B.N., FREUND, J.M., HAN, L., RUBIN, J.P., REING, J.E., JEFFRIES, E.M., WOLF, M.T., TOTTEY, S., BARNES, C.A., RATNER, B.D., & BADYLAK, S.F. (2011). Comparison of three methods for the derivation of a biologic scaffold composed of adipose tissue extracellular matrix. *Tissue Eng Part C Methods*, *17*(4), 411-421. https://doi.org/10.1089/ten.TEC.2010.0342

CANEL, M., SERRELS, A., FRAME, M.C., & BRUNTON, V.G. (2013). E-cadherin-integrin crosstalk in cancer invasion and metastasis. *J Cell Sci*, *126*(Pt 2), 393-401. https://doi.org/10.1242/jcs.100115

CROTTI, S., PICCOLI, M., RIZZOLIO, F., GIORDANO, A., NITTI, D., & AGOSTINI, M. (2017). Extracellular Matrix and Colorectal Cancer: How Surrounding Microenvironment Affects Cancer Cell Behavior? *J Cell Physiol*, *232*(5), 967–975. https://doi.org/10.1002/jcp.25658

DeQUACH, J.A., MEZZANO, V., MIGLANI, A., LANGE, S., KELLER, G. M., SHEIKH, F., & CHRISTMAN, K.L. (2010). Simple and high yielding method for preparing tissue specific extracellular matrix coatings for cell culture. *PLoS One*, *5*(9), e13039. https://doi.org/10.1371/journal.pone.0013039

ERDOGAN, B., & WEBB, D. J. (2017). Cancer-associated fibroblasts modulate growth factor signaling and extracellular matrix remodeling to regulate tumor metastasis. *Biochem Soc Trans*, *45*(1), 229-236. https://doi.org/10.1042/bst20160387

FERNÁNDEZ-PÉREZ, J., & AHEARNE, M. (2019). The impact of decellularization methods on extracellular matrix derived hydrogels. *Sci Rep*, *9*(1), 14933. https://doi.org/10.1038/s41598-019-49575-2

FRANTZ, C., STEWART, K.M., & WEAVER, V.M. (2010). The extracellular matrix at a glance. *J Cell Sci*, *123*(Pt 24), 4195-4200. https://doi.org/10.1242/jcs.023820

FU, R.H., WANG, Y.C., LIU, S.P., SHIH, T.R., LIN, H.L., CHEN, Y.M., SUNG, J.H., LU, C.H., WEI, J.R., WANG, Z.W., HUANG, S.J., TSAI, C.H., SHYU, W.C., & LIN, S.Z. (2014). Decellularization and recellularization technologies in tissue engineering. *Cell Transplant*, *23*(4-5), 621-630. https://doi.org/10.3727/096368914x678382

GILKES, D.M., SEMENZA, G.L., & WIRTZ, D. (2014). Hypoxia and the extracellular matrix: drivers of tumour metastasis. *Nat Rev Cancer*, *14*(6), 430-439. https://doi.org/10.1038/nrc3726

HASHIMOTO, Y., FUNAMOTO, S., SASAKI, S., NEGISHI, J., HATTORI, S., HONDA, T., KIMURA, T., KOBAYASHI, H., & KISHIDA, A. (2019). Re-epithelialization and remodeling of decellularized corneal matrix in a rabbit corneal epithelial wound model. *Mater Sci Eng C Mater Biol Appl*, *102*, 238-246. https://doi.org/10.1016/j.msec.2019.04.024

HOSHIBA, T., CHEN, G., ENDO, C., MARUYAMA, H., WAKUI, M., NEMOTO, E., KAWAZOE, N., & TANAKA, M. (2016). Decellularized Extracellular Matrix as an In Vitro Model to Study the Comprehensive Roles of the ECM in Stem Cell Differentiation. *Stem Cells Int*, *2016*, 6397820. https://doi.org/10.1155/2016/6397820

HOSHIBA, T., LU, H., KAWAZOE, N., & CHEN, G. (2010). Decellularized matrices for tissue engineering. *Expert Opin Biol Ther*, *10*(12), 1717-1728. https://doi.org/10.1517/14712598.2010.534079

KAI, F., DRAIN, A.P., & WEAVER, V.M. (2019). The Extracellular Matrix Modulates the Metastatic Journey. *Dev Cell*, *49*(3), 332–346. https://doi.org/10.1016/j.devcel.2019.03.026

LEE, J.Y., CHANG, J.K., DOMINGUEZ, A.A., LEE, H.P., NAM, S., CHANG, J., VARMA, S., QI, L.S., WEST, R.B., & CHAUDHURI, O. (2019). YAP-independent mechanotransduction drives breast cancer progression. *Nat Commun*, *10*(1), 1848. https://doi.org/10.1038/s41467-019-09755-0

LU, P., WEAVER, V. M., & WERB, Z. (2012). The extracellular matrix: a dynamic niche in cancer progression. *J Cell Biol*, *196*(4), 395-406. https://doi.org/10.1083/jcb.201102147

PICCOLI, M., D'ANGELO, E., CROTTI, S., SENSI, F., URBANI, L., MAGHIN, E., BURNS, A., DE COPPI, P., FASSAN, M., RUGGE, M., RIZZOLIO, F., GIORDANO, A., PILATI, P., MAMMANO, E., PUCCIARELLI, S., & AGOSTINI, M. (2018). Decellularized colorectal cancer matrix as bioactive microenvironment for in vitro 3D cancer research. *J Cell Physiol*, *233*(8), 5937-5948. https://doi.org/10.1002/jcp.26403

ROBINSON, J.R., NEWCOMB, P.A., HARDIKAR, S., COHEN, S.A., & PHIPPS, A.I. (2017). Stage IV colorectal cancer primary site and patterns of distant metastasis. *Cancer Epidemiol*, *48*, 92–95. https://doi.org/10.1016/j.canep.2017.04.003

ROETT, M.A., & EVANS, P. (2009). Ovarian cancer: an overview. *Am Fam Physician*, *80*(6), 609–616.

SHUPE, T., WILLIAMS, M., BROWN, A., WILLENBERG, B., & PETERSEN, B.E. (2010). Method for the decellularization of intact rat liver. *Organogenesis*, *6*(2), 134–136. https://doi.org/10.4161/org.6.2.11546

SIMSA, R., PADMA, A.M., HEHER, P., HELLSTRÖM, M., TEUSCHL, A., JENNDAHL, L., BERGH, N., & FOGELSTRAND, P. (2018). Systematic in vitro comparison of decellularization protocols for blood vessels. *PLoS One*, *13*(12), e0209269. https://doi.org/10.1371/journal.pone.0209269

SOKOLOVA, E.A., VODENEEV, V.A., DEYEV, S.M., & BALALAEVA, I.V. (2019). 3D in vitro models of tumors expressing EGFR family receptors: a potent tool for studying receptor biology and targeted drug development. *Drug Discov Today*, *24*(1), 99–111. https://doi.org/10.1016/j.drudis.2018.09.003

VAROL, C., & SAGI, I. (2018). Phagocyte-extracellular matrix crosstalk empowers tumor development and dissemination. *Febs j*, *285*(4), 734–751. https://doi.org/10.1111/febs.14317

WHITE, L.J., TAYLOR, A.J., FAULK, D.M., KEANE, T.J., SALDIN, L.T., REING, J.E., SWINEHART, I.T., TURNER, N.J., RATNER, B.D., & BADYLAK, S.F. (2017). The impact of detergents on the tissue decellularization process: A ToF-SIMS study. *Acta Biomater*, *50*, 207–219. https://doi.org/10.1016/j.actbio.2016.12.033

WULLKOPF, L., WEST, A.V., LEIJNSE, N., COX, T.R., MADSEN, C.D., ODDERSHEDE, L.B., & ERLER, J.T. (2018). Cancer cells' ability to mechanically adjust to extracellular matrix stiffness correlates with their invasive potential. *Mol Biol Cell*, *29*(20), 2378–2385. https://doi.org/10.1091/mbc.E18-05-0319

YANG, M., CHEN, C.Z., WANG, X.N., ZHU, Y.B., & GU, Y.J. (2009). Favorable effects of the detergent and enzyme extraction method for preparing decellularized bovine pericardium scaffold for tissue engineered heart valves. *J Biomed Mater Res B Appl Biomater*, *91*(1), 354–361. https://doi.org/10.1002/jbm.b.31409